



DOI: <http://dx.doi.org/10.1590/1807-1929/agriambi.v22n4p249-254>

## X-ray computed microtomography in the evaluation of the porous system of soils

Larissa F. Costa<sup>1</sup>, Antonio C. D. Antonino<sup>1</sup>, Richard J. Heck<sup>2</sup>,  
Artur P. Coutinho<sup>3</sup>, Thiago C. Vasconcelos<sup>4</sup> & Cassia B. Machado<sup>5</sup>

<sup>1</sup> Universidade Federal de Pernambuco/Centro de Tecnologia e Geociências/Departamento de Energia Nuclear. Recife, PE. E-mail: larissafcosta@hotmail.com (Corresponding author) - ORCID: 0000-0002-0347-0687; acdantonino@gmail.com - ORCID: 0000-0002-4120-9404

<sup>2</sup> University of Guelph/School of Environmental Sciences. Guelph, Ontario, Canada. E-mail: rheck@uoguelph.ca - ORCID: 0000-0003-4613-439X

<sup>3</sup> Universidade Federal de Pernambuco/Centro Acadêmico do Agreste/Núcleo de Tecnologia. Caruaru, PE. E-mail: arthur.coutinho@yahoo.com.br - ORCID: 0000-0002-5555-4583

<sup>4</sup> Universidade Federal de Pernambuco/Centro de Tecnologia e Geociências/Departamento de Eletrônica e Sistemas. Recife, PE. E-mail: tcampos@gmail.com - ORCID: 0000-0003-3095-8757

<sup>5</sup> Universidade Federal de Pernambuco/Centro de Tecnologia e Geociências/Departamento de Engenharia Civil. Recife, PE. E-mail: cassiabmachado@gmail.com - ORCID: 0000-0001-9993-0678

### Key words:

porosity  
tomographic images  
soil compaction

### ABSTRACT

Analysis of shapes, sizes, continuity, orientation and irregularities of pores can help in the study of soil structural modifications induced by soil management. The study of the inter- and intra-aggregate porous space of urban and rural soils by tomographic images is the objective of this work. A morphometric characterization of the pores was carried out with the analysis of distribution of their size, shape and inclination in these two types of soil. The urban soil showed smaller percentage of inter-aggregate voids and more intra-aggregate voids compared with the rural soil. The cumulative distribution of void volumes showed little pore diversity in the urban soil and great presence of large pores (48%), almost twice the voids with same size in the rural soil. The urban soil, compared to rural soil, also had a higher percentage of flattened pores (29.41%) and a smaller percentage of rounded voids (6.97%), as well as a greater percentage of horizontal voids (44.49%). Hence, the urban soil proved to be more compacted than the rural soil.

### Palavras-chave:

porosidade  
imagens tomográficas  
compactação de solo

## Microtomografia computadorizada de raios X na avaliação do sistema poroso de solos

### RESUMO

A análise dos formatos, tamanhos, continuidade, orientação e irregularidades dos poros pode auxiliar no estudo das modificações estruturais do solo induzidas pelo manejo do solo. O estudo do espaço poroso interagregado e intra-agregado de um solo urbano e de um solo rural por meio de imagens tomográficas é objetivo desse trabalho. Foi feita uma caracterização morfológica dos poros com a análise da distribuição dos tamanhos, formato e inclinação dos poros nesses dois tipos de solo. O solo urbano apresentou menor quantidade de vazios interagregados e maior quantidade de vazios intra-agregados que o solo rural. A distribuição acumulada dos volumes dos vazios apresentou pouca diversidade de poros no solo urbano e grande presença de poros grandes (48%), quase o dobro dos vazios de mesmos tamanhos no solo rural. O solo urbano, quando comparado com solo rural, também apresentou maiores quantidade de poros achatados (29,41%) e menores quantidade de vazios arredondados (6,97%), como também uma maior quantidade de vazios horizontais (44,49%). Com isso, o solo urbano se mostrou estar mais compactado que o solo rural.



## INTRODUCTION

Development of urban areas includes significant leveling and compaction of the soil to support the structures, for instance, bridges, roads, buildings, channels, etc. However, soil compaction is the main limiting factor of water flows, diffusion of substances, soil erosion, carbon and nitrogen cycle, growth of plants and microorganisms, and high costs in the construction of parks and infrastructure works (Chen et al., 2013; Kuncoro et al., 2014a; Zhiyanski et al., 2017).

Characterization of the porous space of a soil provides important indicators in the study on quality and vulnerability of soils subjected to degrading actions related to human activities. Quantification of pore shape, size, continuity, orientation and irregularities can allow the prediction of soil structural modifications induced by human actions, as well as to evaluate soil degradation degree due to compaction and formation of surface crusts (Kuncoro et al., 2014b; Pires et al., 2017). In this context, high-resolution characterization is fundamental to evaluate soil susceptibility to root development, erosion, water storage, water infiltration capacity, among others.

X-Ray computer tomography (CT) is a non-destructive, non-invasive technique that has been successfully used to study soils in 3D since the 1980s (Petrovic et al., 1982; Crestana et al., 1985). Information has been obtained by applying CT to describe and quantitatively measure elements of soil structure, especially characteristics of soil pores and pore network (Taina et al., 2013; Elliot et al., 2010; Soliman et al., 2010; Munkholm et al., 2012).

This study aimed to investigate the differences in porous space between an urban soil and a rural soil through tomographic image analysis. A morphometric characterization was carried out in the pores to analyse the distribution of sizes, shape and inclination, in order to assess quality and degradation level resulting from human activities.

## MATERIAL AND METHODS

Undisturbed sample was collected in the urban soil (US) in the experimental site of the Laboratory of Soil Physics, of the Nuclear Engineering Department of the Federal University of Pernambuco (UFPE), in Recife-PE, Brazil (8° 3' 25.4" S; 34° 57' 19.5" W). Likewise, an undisturbed sample was collected in the rural soil (RS) in the experimental site of the National Observatory of Water and Carbon Dynamics of the Caatinga Biome (ONDACBC), located in the municipality of São João-PE (8° 51' 4.2" S; 36° 22' 56.5" W). Samples were collected in the surface layer using cylindrical PVC samples, diameter x height of 5 x 5 cm for the US, and 7.5 x 7.5 cm for the RS. The analysed samples were dried in the oven at 40 °C. The US is a landfill soil with sandy loam texture in the surface layer, whereas the RS is a Eutrophic Regolithic Neosol, predominantly sandy (Table 1).

Table 1. Physical characterization of the urban and rural soils according to EMBRAPA (2011)

| Sample          | Layer (cm) | Sand Silt Clay     |     |    | Textural class |
|-----------------|------------|--------------------|-----|----|----------------|
|                 |            | g kg <sup>-1</sup> |     |    |                |
| Urban soil - US | 0-20       | 710                | 220 | 70 | Sandy loam     |
| Rural Soil - SR | 0-20       | 880                | 100 | 20 | Sand           |

The tomographic images of the samples were obtained with the third-generation X-ray microtomography system, model NIKON XT H 225 ST, belonging to the research group of the Laboratory of X-ray Computed Tomography (LTCR-X) of the Nuclear Engineering Department of the Federal University of Pernambuco (DEN-UFPE), Brazil. The following parameters were used in the acquisition of the sample: 150 kV tension, 226  $\mu$ A current and 3500 ms exposure time. Spatial resolution was 30  $\mu$ m for US and 50  $\mu$ m for RS. A 0.5-mm-thick copper filter was used to minimize low-intensity photons, which cause beam hardening artifacts.

Images were reconstructed in 3D using the CTPro 3D XT 3.0.3 (Nikon Metrology NV) in a subvolume of interest of 840 x 840 x 840 voxels. In the software VGStudio MAX 2.2 (Volume Graphics, Heidelberg, Germany), the images were converted to the Hounsfield scale, in which the air has value of 0 and water has value of 1000. A 3 x 3 x 3 Gaussian filter was applied to minimize the noises in the images.

Segmentation is the process of distinguishing the regions of interest from the rest of the image. For this study, the region of interest is the soil porous space, and images were segmented into voids and non-voids.

The entire process of image segmentation was executed in the ImageJ 1.50i (Rasband - NIH). The proposed approach is carried out voxel by voxel, and pure voxels were identified and extracted using a plug-in called Pure Voxel Extraction (PVE), which was used to analyse the variability of radiodensity of one voxel with the mean of the values of a 124-voxel neighborhood (window of 5 x 5 x 5 voxels), as proposed by Elliot & Heck (2007a).

A variability threshold coefficient of 20% was adopted for voxel intensity, in comparison to the mean, considering as pure those with intensity within the following interval [ $\mu - 1\sigma$ ,  $\mu + 1\sigma$ ] (Costa et al., 2016). These limits were adopted to locate a multimodal histogram, which can be modeled as a mixture of Gaussians. Since this histogram represents only pure voxels, each Gaussian is associated with one phase of the sample, either voids, matrix or rock fragments, where radiodensity distributions were identified for each phase, through the mean and variance of their respective Gaussians.

The identification and determination of the phases of mixed voxels, based on the means and variance of the phases of interest, were performed by the CT Segmentation plug-in, using four methods: Clamping, Laplacian Filter, Edge Detection and Seeded Region Growing (Elliot & Heck, 2007b; Jefferies et al., 2014).

Voids were analysed using the Particle Analyzer plug-in, present in the ImageJ. This plug-in associates ellipsoids to the voids, providing data such as volume of voxels (pixels<sup>3</sup>), superficial area (pixels<sup>2</sup>), coordinates and size of the reference ellipsoid axes, for instance.

Due to the limited processing capacity of this plug-in to identify and label the many voids existing in one tomographic image of soil, three ranges of size were used: small (S) ( $\leq 8$  voxels), medium (M) ( $< 8$  and  $\geq 100.000$  voxels) and large (L) ( $> 100,000$  voxels) (Costa et al., 2016).

The volume of one void (mm<sup>3</sup>) was calculated by multiplying the volume (in pixel<sup>3</sup> or voxel) by the image resolution (voxel size), according to Eq. 1:

$$V_{\text{void}} = V_{\text{voxel}} \cdot (\text{voxel}^3) \quad (1)$$

For US, voxel size was  $0.03 \times 0.03 \times 0.03 \text{ mm}^3$  and for RS,  $0.05 \times 0.05 \times 0.05 \text{ mm}^3$ . The total volume of voids ( $\geq \text{voxel}$ ) in the analysed subvolumes was determined by the sum of the volumes of S, M and L voids, according to Eq. 2:

$$V_{\text{total}} = \sum V_{\text{void(S)}} + \sum V_{\text{void(M)}} + \sum V_{\text{void(L)}} \quad (2)$$

Porosity was then calculated based on the relationship between total volume of voids ( $\geq \text{voxel}$ ) and the volume of the reconstructed subvolume of the sample, according to Eq. 3:

$$\eta = \frac{V_{\text{total}}}{V_{\text{subvolume}}} \times 100 \quad (3)$$

where,

$$V_{\text{subvolume}} = 840 \times 840 \times 840 \times (\text{voxel}^3) \quad (4)$$

L-type voids were considered as inter-aggregate voids, while voids classified as M and P were considered as the intra-aggregate voids (Costa et al., 2016). Intra-aggregates were classified according to shape, size and inclination. Parameters such as position in the ellipsoid of the shorter axis (Sh), intermediate axis (In) and longer axis (Lg) were calculated by the Particle Analyzer plug-in.

The shape was classified according to the classification of Zingg (1935) and terminologies adopted by Bullock et al. (1985): equant (EQU), prolate (PRO), oblate (OBL) and triaxial (TRI). Due to the complexity of some pores, the plug-in used may not be able to count the voxels constituting one of its axes, making it impossible to determine the shape. These voids were then classified as Without Classification (WC).

Intra-aggregate voids were grouped according to size into microvoids, mesovoids and macrovoids, and subclassified as very wide (vw), wide (w), medium (md), narrow (n) and very narrow (vn) (Passoni et al., 2015). Such sub-classification was performed through a correlation with the volumes occupied by soil grains, such as gravel, sand and silt, according the diameter of an equivalent sphere of these grains, based on classification criteria adopted by Passoni et al. (2015). Hence, the adopted volumes were:  $< \text{vwMicro} \leq 1.598 \times 10^{-5} \text{ mm}^3$ ;  $1.598 \times 10^{-5} < \text{vwMicro} \leq 1.278 \times 10^{-4} \text{ mm}^3$ ;  $1.278 \times 10^{-4} < \text{vnMeso} \leq 1.023 \times 10^{-3} \text{ mm}^3$ ;  $1.023 \times 10^{-3} < \text{nMeso} \leq 8.181 \times 10^{-3} \text{ mm}^3$ ;  $8.181 \times 10^{-3} < \text{mdMeso} \leq 6.545 \times 10^{-2} \text{ mm}^3$ ;  $6.545 \times 10^{-2} < \text{wMeso} \leq 5.230 \times 10^{-1} \text{ mm}^3$ ;  $5.230 \times 10^{-1} < \text{vwMeso} \leq 4.189 \times 10^0 \text{ mm}^3$ ;  $4.189 \times 10^0 < \text{vnMacro} \leq 3.351 \times 10^1 \text{ mm}^3$ ;  $> \text{vnMacro} > 3.351 \times 10^1 \text{ mm}^3$ .

Pore inclination was determined based on Taina et al. (2013), classifying according to the angle between the longest axis of the pore and the axis perpendicular to the soil surface into: quasi-horizontal (QH) ( $75\text{-}105^\circ$ ), inclined-horizontal (IH) ( $60\text{-}75^\circ$  and  $105\text{-}120^\circ$ ), inclined (I) ( $30\text{-}60^\circ$  and  $120\text{-}150^\circ$ ), inclined-vertical (IV) ( $15\text{-}30^\circ$  and  $150\text{-}165^\circ$ ) and quasi-vertical (QV) ( $0\text{-}15^\circ$  and  $165\text{-}180^\circ$ ).

## RESULTS AND DISCUSSION

Table 2 shows the percentage of voids (voxel) identified in the analysed subvolumes of US and RS, approximately 10 and 28% for each soil respectively, of which about 9 and 27% are inter-aggregate voids and about 1 and 0.5% are intra-aggregate voids.

According to Pagliai et al. (2000), a soil is considered as dense or compact when macroporosity ( $> 0.05 \text{ mm}$ ) is lower than 10%, moderately porous for values between 10 and 25%, highly porous when macroporosity varies from 25 to 40%, and extremely porous for values above 40%. Hence, the US can be considered as compact, whereas the RS is highly porous. Reduction in porosity, especially in macroporosity, leads to a reduction in the infiltration rate. A reduction in infiltration rate has negative effects on the environment, because it generates an increase in the volume and coefficient of surface runoff, increasing the frequency of floods in urban areas (Yang & Zang, 2011).

The volume distribution curve for the intra-aggregate voids of the soils is presented in Figure 1. In a curve of this type, its inclination is directly related to the diversity of pores existing in each type of soil, and higher inclination represents greater diversity (Ribeiro et al., 2007). Therefore, the RS showed higher inclination, consequently greater diversity of pores.

The pore distribution curve of US has lower inclination and is concentrated in the lower part of Figure 1, characterizing lower diversity in pore size due to a predominance of larger pores. In the US, more than 48% of intra-aggregate voids are larger than mdMeso, a value equivalent to almost double the percentage of voids with the same size found in the RS ( $\approx 27\%$ ) (Table 3). These types of pores, with diameter larger than  $0.5 \text{ mm}$  (equivalent sphere volume equal to  $0.07 \text{ mm}^3$ ) are directly related to water flow and root penetration, but their large percentage is an indication of poor and harmful structure to plant development (Pagliai & Vignozzi, 2002).

Still according to Pagliai & Vignozzi (2002), pores with diameter between  $0.05$  and  $0.5 \text{ mm}$  (equivalent sphere volume equal to  $6.54 \times 10^{-5} - 0.06545 \text{ mm}^3$ ) are called transmission pores, fundamental for plant nutrition and development. The

Table 2. Porosity of urban soil and rural soil obtained with X-ray computer microtomography

| Sample          | Total voids | Inter-aggregate voids | Intra-aggregate voids |
|-----------------|-------------|-----------------------|-----------------------|
|                 |             | (%)                   |                       |
| Urban Soil – US | 9.97        | 8.93                  | 1.04                  |
| Rural Soil – RS | 28.02       | 27.49                 | 0.53                  |

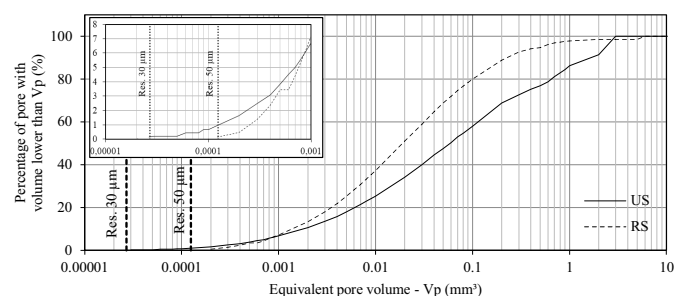


Figure 1. Cumulative distribution curve of intra-aggregate voids of the soils with limitations due to image resolution

Table 3. Distribution of voids within pore size intervals

| Sample          | <vwMicro | vwMicro | vnMeso | nMeso | mdMeso | wMeso | vwMeso | vnMacro | > vnMacro |
|-----------------|----------|---------|--------|-------|--------|-------|--------|---------|-----------|
| Urban Soil – US | 0.00     | 0.93    | 5.79   | 16.39 | 28.52  | 26.50 | 21.88  | 0.00    | 0.00      |
| Rural Soil – RS | 0.00     | 0.46    | 6.74   | 26.23 | 40.00  | 21.90 | 3.26   | 1.40    | 0.00      |

< vwMicro:  $V < 1.598 \times 10^{-5} \text{ mm}^3$ ; vwMicro:  $1.598 \times 10^{-5} < V \leq 1.278 \times 10^{-4} \text{ mm}^3$ ; vnMeso:  $1.278 \times 10^{-4} < V \leq 1.023 \times 10^{-3} \text{ mm}^3$ ; nMeso:  $1.023 \times 10^{-3} < V \leq 8.181 \times 10^{-3} \text{ mm}^3$ ; mdMeso:  $8.181 \times 10^{-3} < V \leq 6.545 \times 10^{-2} \text{ mm}^3$ ; wMeso:  $6.545 \times 10^{-2} < V \leq 5.230 \times 10^{-1} \text{ mm}^3$ ; vwMeso:  $5.230 \times 10^{-1} < V \leq 4.189 \times 10^0 \text{ mm}^3$ ; vnMacro:  $4.189 \times 10^0 < V \leq 3.351 \times 10^1 \text{ mm}^3$ ; vnMacro:  $V > 3.351 \times 10^1 \text{ mm}^3$

US showed approximately 52% of intra-aggregate voids with these dimensions, against about 73% in the RS (Table 3 and Figure 1).

Lower percentage of transmission pores and higher percentage of pores with volume larger than mdMeso may indicate a difficulty for plant development in the US. In addition, greater percentage of pores > mdMeso in the US may result from compaction actions that caused loss of volume and continuity in inter-aggregate voids, transforming them into intra-aggregate voids (Schäffer et al., 2008a, b).

In addition, it was observed an inversion of the cumulative distribution curve of pore volumes in the US (compared with RS), with higher percentages of voids up to  $0.0009 \text{ mm}^3$  and lower percentages of voids >  $0.0009 \text{ mm}^3$  (Figure 1). This behavior, according to Lipiec et al. (2012), may represent a higher compaction of this soil.

The zero value found for the voids < vwMicro in both soils (Table 3) does not mean their inexistence, but a limitation of the technique to identify them due to the resolutions adopted in the scanning and reconstruction of images. In the US, with 30- $\mu\text{m}$  resolution, it was only possible to analyse voids larger than  $2.7 \times 10^{-5} \text{ mm}^3$  and in the RS, due to the 40  $\mu\text{m}$  resolution, it was only possible to analyse voids larger than  $1.25 \times 10^{-4} \text{ mm}^3$ . Both limits that can be analysed are larger than  $1.598 \times 10^{-5} \text{ mm}^3$ , maximum volume for voids classified as < vwMicro (Figure 1).

For the shape of intra-aggregate voids (Figure 2), the US showed lower percentage of EQU and PRO voids, in comparison to the RS. The presence of these voids may be an indication of soil quality, because they are related to biological activities in this environment (Carducci et al., 2014). Hence, the US may exhibit a more deficient development of plants and animals, compared with the RS.

The flattening of a pore may be related to a compaction process of a medium, since the force exerted on it may generate its compression (Schäffer et al., 2008a, b). According to Arasan

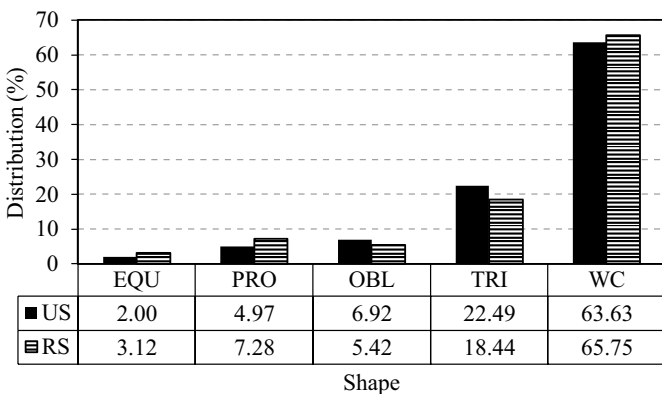


Figure 2. Distribution of shapes of intra-aggregate voids in the urban soil and rural soil

et al. (2011), the TRI and OBL shapes are characterized for being more flattened than EQU and PRO. Since the US showed higher percentage of EQU and OBL voids, it may indicate a more compacted medium.

Voids without classification may be related to the complexity of pore shape, being associated with root development, wetting and drying cycles, human actions and biota (Pires et al., 2017). The US showed lower pore complexity, which may result from its greater compaction, leading to lower root development and reduction in water infiltration rate.

Comparing the inclination of intra-aggregate voids of the studied soils, there was higher percentage of QV, IV and I voids in the RS, and higher percentage of IH and QH in the US (Figure 3). Pore horizontality indicates higher resistance to root penetration, i.e., higher soil compaction. Pore verticality is associated with a soil without physical barriers for root proliferation or activities of animals, such as earthworms. Pore inclination and tortuosity represent the need for root branching in the search for nutrients and water. In addition, pore inclination is strongly related to water infiltration in the soil; horizontal pores, especially on soil surface, lead to a significant reduction in water infiltration (Jassogne et al., 2007).

Both soils studied showed higher percentage of IH and QH pores, totaling approximately 58 and 52% in US and RS, respectively. In RS, the predominance of these types of voids is due to the presence of clay bands, also called lamellae, which are horizontal, thin, discontinuous, clay-rich layers associated or not with Fe oxides (Almeida et al., 2015). In the US, this horizontality of voids results from the compaction of this medium, due to the need to increase its resistance.

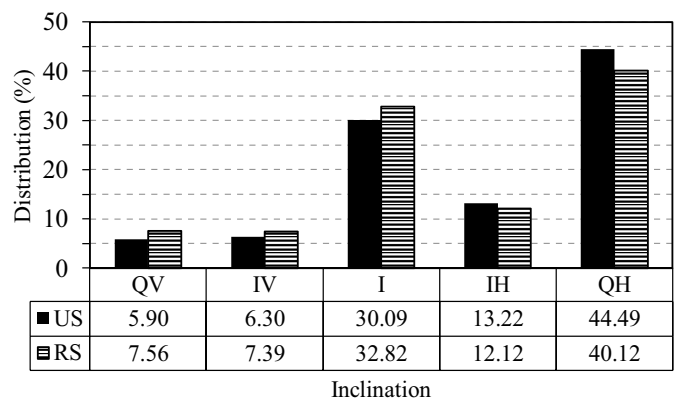


Figure 3. Distribution of the inclinations of intra-aggregate voids in urban soil and rural soil

### CONCLUSIONS

1. Compared with the rural soil, the urban soil showed lower percentage of inter-aggregate voids and higher percentage of intra-aggregate voids, with low diversity of pore size.

2. The urban soil showed higher percentages of flattened pores, round pores and horizontal voids, in comparison to the rural soil.

3. X-ray computed microtomography allowed to identify, non-invasively, the differences between the porous space structures of an urban soil and a rural soil, evidencing that the urban soil is more compacted than the rural soil.

### ACKNOWLEDGMENTS

To the National Council for Scientific and Technological Support (CNPq) for the support to the research, by providing the Master's scholarship to the first author (Process N°. 130874/2015-9) and Productivity Grant to the second author. To the LTCR-X (DEN-UFPE) for providing the microtomography, server and programs used in the acquisition and analyses of the images.

### LITERATURE CITED

- Almeida, A. van der L. de; Corrêa, M. M.; Lima, J. R. de S.; Souza, E. S. de; Santoro, K. R.; Antonino, A. C. D. Atributos físicos, macro e micromorfológicos de neossolos regolíticos no agreste meridional de Pernambuco. *Revista Brasileira de Ciência do Solo*, v.39, p.1235-1246, 2015. <https://doi.org/10.1590/01000683rbc20140757>
- Arasan, S.; Akbulut, S.; Hasioglu, A. S. Effect of particle size and shape on the grain-size distribution using image analysis. *International Journal of Civil & Structural Engineering*, v.1, p.968-985, 2011.
- Bullock, P.; Fedoroff, N.; Jongerius, A.; Stoops, G.; Tursina, T. Handbook for soil thin section description. Albrington: Waine Research, 1985. 152p.
- Carducci, C. E.; Oliveira, G. C. de; Curi, N.; Heck, R. J.; Rossoni, D. F. Scaling of pores in 3D images of Latosols (Oxisols) with contrasting mineralogy under a conservation management system. *Soil Research*, v.52, p.231-243, 2014. <https://doi.org/10.1071/SR13238>
- Chen, Y.; Day, S. D.; Wick, A. F.; Strahm, B. D.; Wiseman, P. E.; Daniels, W. L. Changes in soil carbon pools and microbial biomass from urban land development and subsequent post-development soil rehabilitation. *Soil Biology and Biochemistry*, v.66, p.38-44, 2013. <https://doi.org/10.1016/j.soilbio.2013.06.022>
- Costa, L. F.; Antonino, A. C. D.; Heck, R. J.; Coutinho, A. P.; Mendonça Pimentel, R. M. de; Vasconcelos, T. C.; Machado, C. B. Espaço poroso em solos brasileiros usando tomografia computadorizada de raios-X. *Revista Brasileira de Geografia Física*, v.9, p.692-706, 2016. <https://doi.org/10.5935/1984-2295.20160047>
- Crestana, S.; Mascarenhas, S.; Pozzi-Mucelli, R. S. Static and dynamic three-dimensional studies of water in soil using computed tomographic scanning. *Soil Science*, v.140, p.326-332, 1985. <https://doi.org/10.1097/00010694-198511000-00002>
- Elliot, T. R.; Heck, R. J. A comparison of optical and X-ray technique for void analysis in soil thin section. *Geoderma*, v.141, p.60-70, 2007a. <https://doi.org/10.1016/j.geoderma.2007.05.001>
- Elliot, T. R.; Heck, R. J. A comparison of 2D vs 3D thresholding of X-ray CT imagery. *Canadian Journal of Soil Science*, v.87, p. 405-412, 2007b. <https://doi.org/10.4141/CJSS06017>
- Elliot, T. R.; Reynolds, W. D.; Heck, R. J. Use of existing pore models and X-ray computed tomography to predict saturated soil hydraulic conductivity. *Geoderma*, v.156, p.133-142, 2010. <https://doi.org/10.1016/j.geoderma.2010.02.010>
- EMBRAPA - Empresa Brasileira de Pesquisa Agropecuária. Manual de métodos de análise de solos. Rio de Janeiro: Embrapa Solos, v.2, 2011. 230p.
- Jassogne, L.; McNeill, A.; Chittleborough, D. 3D-visualization and analysis of macro-and meso-porosity of the upper horizons of a sodic, texture-contrast soil. *European Journal of Soil Science*, v.58, p.589-598, 2007. <https://doi.org/10.1111/j.1365-2389.2006.00849.x>
- Jefferies, D. A.; Heck, R. J.; Thevathasan, N. V.; Gordon, A. M. Characterizing soil surface structure in a temperate tree-based intercropping system using X-ray computed tomography. *Agroforestry Systems*, v.88, p.645-656, 2014. <https://doi.org/10.1007/s10457-014-9699-0>
- Kuncoro, P. H.; Koga, K.; Satta, N.; Muto, Y. A study on the effect of compaction on transport properties of soil gas and water I: Relative gas diffusivity, air permeability, and saturated hydraulic conductivity. *Soil and Tillage Research*, v.143, p.172-179, 2014a. <https://doi.org/10.1016/j.still.2014.02.006>
- Kuncoro, P. H.; Koga, K.; Satta, N.; Muto, Y. A study on the effect of compaction on transport properties of soil gas and water. II: Soil pore structure indices. *Soil and Tillage Research*, v.143, p.180-187, 2014b. <https://doi.org/10.1016/j.still.2014.01.008>
- Lipiec, J.; Hajnos, M.; Swieboda, R. Estimating effects of compaction on pore size distribution of soil aggregates by mercury porosimeter. *Geoderma*, v.179, p.20-27, 2012. <https://doi.org/10.1016/j.geoderma.2012.02.014>
- Munkholm, L. J.; Heck, R. J.; Deen, B. Soil pore characteristics assessed from X-ray micro-CT derived images and correlations to soil friability. *Geoderma*, v.181-182, p.22-29, 2012. <https://doi.org/10.1016/j.geoderma.2012.02.024>
- Pagliai, M.; Pellegrini, S.; Vignozzi, N.; Rouseva, S.; Grasselli, O. The quantification of the effect of subsoil compaction on soil porosity and related physical properties under conventional to reduced management practices. *Advances in GeoEcology*, v.32, p.305-313, 2000.
- Pagliai, M.; Vignozzi, N. The soil pore system as an indicator of soil quality. *Advances in GeoEcology*, v.35, p.69-80, 2002.
- Passoni, S.; Pires, L. F.; Heck, R. J.; Rosa, J. A. Three dimensional characterization of soil macroporosity by x-ray microtomography. *Revista Brasileira de Ciência do Solo*, v.39, p.448-457, 2015. <https://doi.org/10.1590/01000683rbc20140360>
- Petrovic, A. M.; Siebert, J. E.; Rieke, P. E. Soil bulk density analysis in three dimensions by computed tomographic scanning. *Soil Science Society of America Journal*, v.46, p.445-450, 1982. <https://doi.org/10.2136/sssaj1982.03615995004600030001x>
- Pires, L. F.; Borges, J. A. R.; Rosa, J. A.; Cooper, M.; Heck, R. J.; Passoni, S.; Roque, W. L. Soil structure changes induced by tillage systems. *Soil and Tillage Research*, v.165, p.66-79, 2017. <https://doi.org/10.1016/j.still.2016.07.010>
- Ribeiro, K. D.; Menezes, S. M.; Mesquita, M. da G. B. de F. Sampaio, F. de M. T. Propriedades físicas do solo, influenciadas pela distribuição de poros, de seis classes de solos da região de Lavras-MG. *Ciência e Agrotecnologia*, v.31, p.1167-1175, 2007. <https://doi.org/10.1590/S1413-70542007000400033>

- Schäffer, B.; Mueller, T. L.; Stauber, M.; Müller, R.; Keller, M.; Schulin, R. Soil and macro-pores under uniaxial compression. II. Morphometric analysis of macro-pore stability in undisturbed and repacked soil. *Geoderma*, v.146, p.175-182, 2008a. <https://doi.org/10.1016/j.geoderma.2008.05.020>
- Schäffer, B.; Stauber, M.; Mueller, T. L.; Müller, R.; Schulin, R. Soil and macro-pores under uniaxial compression. I. Mechanical stability of repacked soil and deformation of different types of macro-pores. *Geoderma*, v.146, p.183-191, 2008b. <https://doi.org/10.1016/j.geoderma.2008.05.019>
- Soliman, A. S.; Abdel-Rahman, M. E.; Heck, R. J. Comparing time-resolved infrared thermography and X-ray computed tomography in distinguishing soil surface crusts. *Geoderma*, v.158, p.101-109, 2010. <https://doi.org/10.1016/j.geoderma.2010.02.008>
- Taina, I. A.; Heck, R. J.; Deen, W.; Ma, E. Y. T. Quantification of freeze-thaw related structure in cultivated topsoils using X-ray computer tomography. *Canadian Journal of Soil Science*, v.93, p.533-553, 2013. <https://doi.org/10.4141/cjss2012-044>
- Yang, J.-L.; Zhang, G.-L. Water infiltration in urban soils and its effects on the quantity and quality of runoff. *Journal of Soils and Sediments*, v.11, p.751-761, 2011. <https://doi.org/10.1007/s11368-011-0356-1>
- Zhiyanski, M.; Sokolovska, M.; Glushkova, M.; Vilhar, U.; Lozanova, L. The urban forest: Cultivating green infrastructure for people and the environment. *Soil Quality*, v.7, p.49-58, 2017.
- Zingg, T. Beiträge zur Schotteranalyse. *Schweizer Mineralogische und Petrographische Mitteilungen*, v.15, p.39-140, 1935.